Kinesin Steps Do Not Alternate in Size

Adrian N. Fehr,* Charles L. Asbury,‡ and Steven M. Block*†
Departments of *Applied Physics and †Biological Sciences, Stanford University, Stanford, California 94305; and ‡Department of Physiology & Biophysics, University of Washington, Seattle, Washington 98195

ABSTRACT Kinesin is a two-headed motor protein that transports cargo inside cells by moving stepwise on microtubules. Its exact trajectory along the microtubule is unknown: alternative pathway models predict either uniform 8-nm steps or alternating 7- and 9-nm steps. By analyzing single-molecule stepping traces from "limping" kinesin molecules, we were able to distinguish alternate fast- and slow-phase steps and thereby to calculate the step sizes associated with the motions of each of the two heads. We also compiled step distances from nonlimping kinesin molecules and compared these distributions against models predicting uniform or alternating step sizes. In both cases, we find that kinesin takes uniform 8-nm steps, a result that strongly constrains the allowed models.

Received for publication 16 October 2007 and in final form 7 December 2007.

Address reprint requests and inquiries to Steven M. Block, Tel.: 650-724-4046; Fax: 650-723-6132;
E-mail: sblock@stanford.edu.

Conventional kinesin is a homodimeric motor protein with two microtubule-binding head domains linked to a common, coiled-coil stalk. It moves processively, taking up to hundreds of steps along microtubules before dissociating (1). Kinesin steps are produced by an asymmetric, hand-over-hand walk carried out by its heads (2–4) as it follows a path parallel to the microtubule protofilaments (5). However, the trajectories followed by the heads during stepping have long been a source of controversy (6–9), and remain an outstanding issue in the field (10). Using a high-resolution optical trapping assay, we measured the positions of microscopic beads attached to the stalks of single kinesin molecules, and from these data inferred the motions of the heads. It is not yet well established whether kinesin spends time during stepping in a predominantly one-head-bound state (8,10) or in a two-heads-bound state (4,11), so both possibilities were considered. For the case where kinesin molecules dwell mainly in a one-head-bound state, there are two plausible stepping scenarios (Fig. 1): the ''tightrope'' pathway, where successive microtubule binding sites and stalk positions both lie along a common line coincident with a single protofilament of the microtubule surface lattice, and the ''straddle'' pathway, where successive microtubule binding sites alternate between adjacent protofilaments and the stalk position follows a zigzag pathway among these positions. In the tightrope pathway, the stalk advances by uniform, 8-nm steps as the heads move from one tubulin dimer to the next. In the straddle pathway, however, due to the ~1-nm longitudinal offset between adjacent protofilaments (12), the stalk advances alternately in ~7- and ~9-nm steps, measured as projections along the microtubule axis. For the case where kinesin molecules dwell predominantly in a two-heads-bound state, the tightrope pathway generates uniform, 8-nm steps. In contrast, the straddle pathway can lead, in principle, either to uniform 8-nm steps (the ''normal straddle'', corresponding to the situation where the stalk position reports the average location of the two bound heads) or to a zigzag motion with alternating step sizes, just as above (the ''asymmetric straddle'', corresponding to the situation where the kinesin stalk is pulled closer to one head than to the other).

We used an optical force-clamp apparatus with high spatiotemporal resolution to measure the stepping motions of single kinesin molecules attached to 0.5-μm diameter beads, which were trapped in solution, then placed near coverslip-immobilized microtubules (2). Once a kinesin molecule bound the microtubule and began moving processively, a feedback loop was automatically engaged to maintain a fixed separation between the bead and the trap center, thereby applying constant load to the kinesin molecule. Records of the positions of beads obtained under such conditions displayed a clear series of molecular steps, with abrupt transitions lasting <2 ms. Operationally, the step distance was calculated from the difference in the mean positions of dwell intervals located on either side of a given transition (Supplementary Material). In principle, a careful comparison of the distances subtended by the even- and odd-numbered steps within a single, long record of kinesin motion could be used to discriminate among the competing pathway models. In practice, however, positional noise within individual records (SD ~2 nm; $N = 1{,}063$) and the reduced processivity of kinesin molecules under load (which limits the number of steps before dissociation) preclude such an approach. Instead, statistical accuracy was improved by combining data from many different runs and molecules. The challenge, then, is to find a way to keep track of the phases of alternating steps between records. This challenge was met by collecting data from force-clamped recombinant kinesin molecules (load $= -4$ pN; [ATP] $= 2$ mM) that display an

Editor: Yale E. Goldman.

doi: 10.1529/biophysj.107.126839

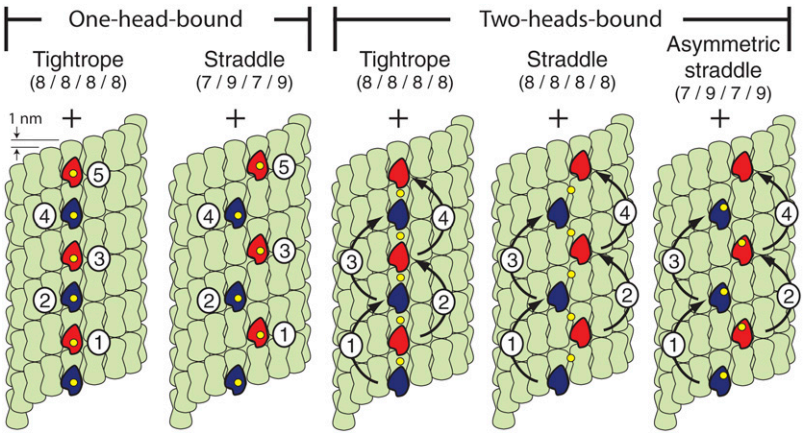

FIGURE 1 Stepping pathways. Candidate trajectories for kinesin stepping predict consecutive 8-nm steps or alternating 7- and 9-nm steps, measured along the microtubule axis from a point on the stalk. The surface lattice for a 13-protofilament microtubule and successive positions (numbered) occupied by the walking heads (*red* and *blue*) of a dimeric kinesin molecule are shown. Stalk position is indicated (*yellow*), along with head motions (*black arrows*). Tubulin α-β heterodimers (*green dumbbells*) form longitudinal protofilaments that are offset by 0.94 nm. In one-head-bound models, the position of the free head is not displayed; the stalk reports a position near the bound head. For the tightrope and straddle models, the stalk position is assumed to be located at the midpoint between the bound heads; in the asymmetric straddle model, the stalk is associated with a single head.

intrinsic asymmetry in their stepping behavior, and therefore provide a means of distinguishing their alternating steps, i.e., by using molecules that limp (2).

The timing of the successive steps taken by a recombinant, homodimeric kinesin molecule (DmK401) has previously been shown to alternate between fast and slow rates (2). Assuming that the slow and fast dwell times correspond to the alternating motions of its two heads in a hand-over-hand walk (2–4), we can sort kinesin steps on this basis and thereby combine data from multiple records. We separately computed the average duration of all even- and odd-numbered dwell times within every record, assigning those times with shorter average duration to the ''fast'' phase and times with longer average duration to the ''slow'' phase. As found previously, the distributions of the fast and slow phases assigned in this way were fit by exponentials with different time constants (2), implying that the two classes of step arise from distinct stochastic processes. The severity of limping for each record was assessed by its limp factor, L, defined as the ratio of the average slow step duration to the average fast step duration for records containing $\geq$6 dwell intervals. Stepping traces were analyzed as described, and records with $L \geq 5$ were retained for analysis (Supplementary Material; $N = 107$ records; 10 beads). Average step sizes associated with either the fast or slow phases were statistically indistinguishable (two-tailed t-test; $t = 0.27$; $\alpha = 0.05$; $P < 0.001$) and well-fit by Gaussians with means of 8.20 nm (Fig. 2 *a*). The average step size here is identical to previous measurements for kinesin based on the motions produced by both heads (13).

We also compiled step data from nonlimping, wild-type kinesin molecules (LpK) purified from squid optic lobe under force-clamped conditions (load = –5 pN; [ATP] = 2 mM). Because phase assignments cannot be made in the absence of limping, the histogram of all step distances was tested against fits to alternative models (Fig. 2 *b*): 1), a single Gaussian distribution or 2), a sum of two Gaussian distributions with fixed means (7.28 nm; 9.16 nm), equal to the experimental best-fit kinesin step size (8.22 nm) increased and decreased by the longitudinal offset between adjacent protofilaments (the stagger distance). For microtubules with a B-type helical lattice, the offset is given by (3/13) times the axial monomer spacing for a 13-protofilament, 3-start helical microtubule (14). Based on x-ray and electron diffraction, estimates of the monomer spacing range from 4.05 to 4.09 nm (12,15,16), corresponding to a stagger distance of ~0.94 nm. Fitting returned ($\chi^2_\nu = 1.68$; $\nu = 7$; $P \sim 0.15$) for a single Gaussian and ($\chi^2_\nu = 5.02$; $\nu = 6$; $P <$

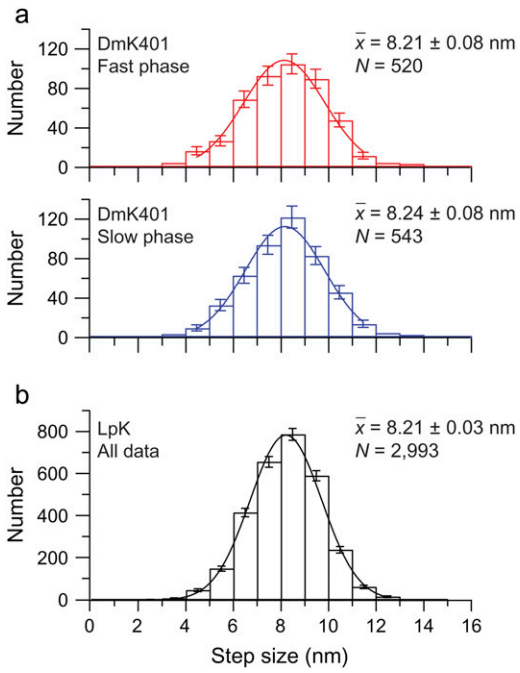

FIGURE 2 Step size distributions and Gaussian fits. (*a*) DmK401 histograms of sizes for the fast (*red bars*) and slow (*blue bars*) phases with superposed Gaussian fits (*solid lines*); bin width 1 nm; statistical errors as indicated. Best fit values ($\mu \pm \sigma_\mu$) are 8.19 ± 0.09 nm (*red*) and 8.22 ± 0.08 nm (*blue*). (*b*) LpK distribution of all step sizes (*black bars* with statistical errors). Data are fit to a Gaussian (*solid line*) with 8.22 ± 0.03 nm ($\mu \pm \sigma_\mu$). All fits were restricted to bins with $\geq$10 counts. Legends display sample averages mean ± SE.

0.001) for two offset Gaussians. Comparing these results by an F-test (17), we find that the experimental data from native kinesin are more likely to represent a single step size than two (alternating) step sizes ($F = 3.0$; $P = 0.09$).

Control experiments confirmed that both analytical methods report alternating step sizes of ~7 and ~9 nm when actually present. Kinesin-coated beads were immobilized on microtubules using a nonhydrolyzable ATP analog. To simulate stepping, the microscope piezo stage was advanced in alternating 7- and 9-nm increments at random times chosen from exponential distributions. Alternating step sizes were faithfully recovered (Supplementary Material). These simulated data were also fit to either one or two Gaussians, as described in the foregoing: in this instance, the fit to two Gaussians was superior (F-test: $F = 5.2$; $P = 0.04$).

Previous work that tracked at nanometer-level accuracy the position of a single fluorophore attached to one of the two kinesin heads revealed steps of ~16 nm during processive movement (i.e., alternating steps of 0 and 16 nm for a given labeled head) (4). This result may be taken as evidence that both kinesin heads are likely to be localized to different sites on the microtubule throughout most of the kinetic cycle, as opposed to one being freely tethered or closely associated with its partner. Additional support for this interpretation came from FRET-based experiments conducted with dyes placed on the kinesin stalk and one head, which were most consistent with a two-heads-bound intermediate state during stepping (18). Recent evidence that the rear head of kinesin may be able to synthesize ATP under certain conditions also suggests that both its heads remain predominantly bound to the microtubule during the stepping cycle (11). These observations argue against one-head-bound pathway models (Fig. 1).

By contrast, Cross and co-workers (19) recently concluded that dimeric kinesin molecules can bind to individual α-β tubulin dimers not formed into protofilaments. Results of their biochemical kinetic experiments, conducted with such tubulin-bound motors, suggested that one kinesin head may be able to regulate the biochemical cycle of its partner even under conditions where both heads are not simultaneously bound to a common substrate. These findings were therefore interpreted as lending support to a one-head-bound trajectory, where a tethered head spends significant time ''docked'' against its bound partner during the stepping cycle. However, it is not clear whether the conclusions reached by Cross and colleagues relate to normal processive stepping, or perhaps may represent a new form of head ''gating'' peculiar to tubulin dimers, as pointed out in an accompanying commentary (20).

We conclude that kinesin molecules step invariably by 8 nm during processive motion, as measured from a point on the common stalk: this point does not alternate between 7- and 9-nm advancements. Our finding therefore excludes pathway models that require such alternation, i.e., the one-head-bound straddle model and the two-heads-bound asymmetric straddle model (Fig. 1). Taking the available experimental evidence into consideration, we tend to favor a two-heads-bound pathway, and therefore propose that kinesin steps either by a two-heads-bound tightrope or by a two-heads-bound straddle mechanism. Future experiments may be able to discern additional features of kinesin motion that would distinguish between these alternatives.

SUPPLEMENTARY MATERIAL

To view the supplemental file associated with this article, visit www.biophysj.org.

We acknowledge support from a National Science Foundation Graduate Research Fellowship (A.N.F.) and National Institutes of Health grant R01-GM51453 (S.M.B.).

REFERENCES and FOOTNOTES

1. Howard, J., A. J. Hudspeth, and R. D. Vale. 1989. Movement of microtubules by single kinesin molecules. *Nature*. 342:154–158.
2. Asbury, C. L., A. N. Fehr, and S. M. Block. 2003. Kinesin moves by an asymmetric hand-over-hand mechanism. *Science*. 302:2130–2134.
3. Kaseda, K., H. Higuchi, and K. Hirose. 2003. Alternate fast and slow stepping of a heterodimeric kinesin molecule. *Nat. Cell Biol.* 5:1079–1082.
4. Yildiz, A., M. Tomishige, R. D. Vale, and P. R. Selvin. 2004. Kinesin walks hand-over-hand. *Science*. 303:676–678.
5. Ray, S., E. Meyhofer, R. A. Milligan, and J. Howard. 1993. Kinesin follows the microtubule's protofilament axis. *J. Cell Biol*. 121:1083–1093.
6. Block, S. M., and K. Svoboda. 1995. Analysis of high resolution recordings of motor movement. *Biophys. J*. 68:2305S–2395S (discussion 2395S–2415S).
7. Lockhart, A., I. M. T. C. Crevel, and R. A. Cross. 1995. Kinesin and NCD bind through a single head to microtubules and compete for a shared MT binding site. *J. Mol. Biol*. 249:763–71.
8. Cross, R. A. 1995. On the hand-over-hand footsteps of kinesin heads. *J. Muscle Res. Cell Motil.* 16:91–94.
9. Block, S. 1998. Kinesin: what gives? *Cell*. 93:5–8.
10. Cross, R. A. 2004. Molecular motors: kinesin's interesting limp. *Curr. Biol.* 14:R158–R159.
11. Hackney, D. D. 2005. The tethered motor domain of a kinesin-microtubule complex catalyzes reversible synthesis of bound ATP. *Proc. Natl. Acad. Sci. USA*. 102:18338–18343.
12. Mandelkow, E., J. Thomas, and C. Cohen. 1977. Microtubule structure at low resolution by x-ray diffraction. *Proc. Natl. Acad. Sci. USA*. 74:3370–3374.
13. Svoboda, K., C. F. Schmidt, B. J. Schnapp, and S. M. Block. 1993. Direct observation of kinesin stepping by optical trapping interferometry. *Nature*. 365:721–727.
14. Chretien, D., and R. H. Wade. 1991. New data on the microtubule surface lattice. *Biol. Cell*. 71:161–174.
15. Li, H., D. J. DeRosier, W. V. Nicholson, E. Nogales, and K. H. Downing. 2002. Microtubule structure at 8 Å resolution. *Structure*. 10:1317–1328.
16. Wais-Steider, C., N. S. White, D. S. Gilbert, and P. A. Eagles. 1987. X-ray diffraction patterns from microtubules and neurofilaments in axoplasm. *J. Mol. Biol*. 197:205–218.
17. Bevington, P. R., and D. K. Robinson. 1992. Data Reduction and Error Analysis for the Physical Sciences. WCB/McGraw-Hill, New York.
18. Tomishige, M., N. Stuurman, and R. D. Vale. 2006. Single-molecule observations of neck linker conformational changes in the kinesin motor protein. *Nat. Struct. Mol. Biol.* 13:887–894.
19. Alonso, M. C., D. R. Drummond, S. Kain, J. Hoeng, L. Amos, and R. A. Cross. 2007. An ATP gate controls tubulin binding by the tethered head of kinesin-1. *Science*. 316:120–123.
20. Hackney, D. D. 2007. Biochemistry. Processive motor movement. *Science*. 316:58–59.

Supplementary Material for

Kinesin steps do not alternate in size

Adrian N. Fehr, Charles L. Asbury and Steven M. Block
Corresponding author: Steven M. Block, Tel.: 650-724-4046; Fax: 650-723-6132; E-mail: sblock@stanford.edu.

Supplementary Methods

Single-molecule optical trapping assays with recombinant and native kinesin were conducted at saturating ATP levels (2 mM) using protocols described previously (Asbury et al., 2003, *Kinesin moves by an asymmetric hand-over-hand mechanism*. ***Science*** **302**: 2130-2134). Truncated, recombinant conventional kinesin (Kinesin-1) from *Drosophila melanogaster*, DmK401, was expressed and clarified by centrifugation as previously described (*Ibid.*). Clarified lysate was then mixed 1:4 with binding buffer (50 mM $NaPO_4$, 60 mM imidazole, 250 mM NaCl, 1 mM $MgCl_2$, 2 mM DTT, 10 μM ATP, pH 8.0) and incubated on His-binding columns (HisTrap FF Crude; GE Healthcare, Piscataway, NJ) at 4°C for 8 hours. Using an FPLC, columns were washed (wash buffer is identical to binding buffer, but adjusted to pH 6.0) and kinesin protein was eluted with an imidazole gradient (elution buffer is identical to binding buffer contains 0.5 M imidazole and is adjusted to pH 7.0). Kinesin fractions were monodisperse, as judged by SDS-PAGE gels, and stored in 50% glycerol at -20°C until use. Native, conventional squid kinesin was also purified from optic lobes of *Loligo pealii* and used as described (*Ibid.*).

During force-clamped kinesin stepping experiments, position data were acquired at 20 kHz, decimated to 2 kHz and then filtered at the appropriate Nyquist frequency (1 kHz) with a 6-pole Bessel filter. Under our assay conditions (temperature 21.2° C), the mean kinesin speeds at the retarding forces used (~150 nm/s) imply an average dwell time of ~50 ms. Hence, the vast majority of kinesin dwell intervals could be clearly resolved beyond the thermal noise (see Fig. S1). These events were identified and scored using an automated step-finding algorithm written in Igor Pro 5.0 (WaveMetrics, Lake Oswego, OR). All stepping transitions identified in this fashion were subsequently confirmed by eye, and adjusted if necessary. Note that for the determination of stepping *distances* (in contrast to stepping *times*), the measurement of records is fairly robust against any small errors made in the precise determination of the locations of stepping transitions, because the positional average for each dwell interval is dominated by the

majority of data found in the plateau region for each step, and not by the transient changes that occur at the step boundaries. To be included for analysis, we required a minimum duration of 4 ms for a dwell interval. For the purpose of this study, we assumed that any brief, 16-nm displacements simply corresponded to back-to-back 8-nm steps that were unresolved, and therefore were disregarded. Such events were rare (<5% of all steps). Details of our step-finding algorithm are found in the Appendix to the Supplemental Material. For a recent discussion of the performance of step-finding algorithms, please refer to (Carter, B.C., Vershinin, M., and S.P. Gross, *A comparison of step-detection methods: how well can you do?* ***Biophys. J.***, 2007, ePub ahead of publication doi:10.1529/biophysj.107.110601). The code to our algorithm, and to other routines produced by our laboratory for this work, is available upon request.

Fits to models consisting of either one or two Gaussian distributions were compared statistically by means of the *F*-test, which is based on the ratio of reduced chi-squared values (i.e., chi-squared divided by the number of degrees of freedom) for the two candidate distributions (see, for example, Bevington, P. R., and D. K. Robinson. 1992. *Data Reduction and Error Analysis for the Physical Sciences*. 2nd Edn. McGraw-Hill, New York.). Implicit in the use of the *F*-test is the assumption that experimental deviations from the parent (model) function follow the usual chi-square distribution, which in turn requires that errors at data points be normally distributed. Counting errors computed for individual histograms bins were taken to be statistical errors (i.e., equal to $\sqrt{N}$, where N is the number of counts). The distributions of such counting errors are very well approximated by the normal distribution whenever $N \geq 10$. Bins with $N < 10$ counts were excluded from fits (Legend to Fig. 2).

Supplementary Data 1: Phase assignment errors. For a kinesin molecule that steps with alternating stochastic dwell times that differ by a factor of ~5, on average, there is a finite probability that in records containing small numbers of steps, the "slow" phase will appear to be faster than the "fast" phase, due to limited sampling. To test the effect of this sampling error on our measurements, we created simulated stepping records *in silico* with exponentially-distributed numbers of steps (mean = 5 steps) and sequential dwell times drawn from exponential distributions with different time constants, similar to those values previously found in actual limping kinesin records (Asbury et al., 2003, ***Science*** **302**: 2130-2134). We found that the stochastic nature of stepping caused relatively few mistakes in assignment: 350 errors per

50,000 records, or 0.7%. However, this represents a best-case scenario, because it remains possible that a small percentage of steps are not resolved in a given record, which would cause the phase to be lost, and thereby increase the error rate. Missing a step effectively lowers the limp factor for that record however. Therefore, we excluded runs with $L < 5$ and redid the simulations, and found that the error rate was thereby reduced to ~2 per 50,000 records, or 0.004%. Setting the threshold in this manner therefore reduces the possibility of missed phase assignments to negligible levels.

Supplementary Data 2: Stepping controls. To determine if these experiments supplied sufficient resolving power to distinguish alternating steps separated by ~2 nm, we performed a hardware-based simulation of kinesin stepping. Beads carrying limiting numbers of kinesin molecules (diluted to a limit where only a single molecule would bind) were immobilized on microtubules using the non-hydrolyzable ATP analog, AMP-PNP. Records of bead position were then collected using our standard force-clamp software as the piezoelectric stage position was moved in alternating 6.9- and 9.1-nm increments under computer control (in effect, pulling the kinesin/bead across the detection region as a kinesin molecule normally would), with sequential dwell times drawn from exponential distributions with two different time constants (Fig. S2 *A*). Position data were analyzed in a manner identical to normal kinesin stepping data. After separating steps by phase, we found that the slow and fast components corresponded to steps measuring 7.1 ± 0.1 nm ($N = 419$) and 9.3 ± 0.1 nm ($N = 420$), respectively (Fig. S2 *B*), consistent with the input parameters. We also pooled all step sizes and fitted these data with both a single Gaussian (with fixed mean of 8.2 nm) and a double-Gaussian (with fixed means of 6.9 and 9.1 nm). We found that the $\chi^2_\nu = 9.8$; $N = 7$; $P \sim 0.001$ for the Gaussian and $\chi^2_\nu = 1.9$; $N = 7$; $P \sim 0.1$ for two Gaussians ($F = 5.2$; $P = 0.05$), again consistent with steps being drawn from a parent distribution with two step sizes, not one.

Figure S1: Representative stepping records for three DmK401 molecules. Limping motion is apparent as alternating slow and fast dwell intervals, scored by an automated algorithm and colored blue and red, respectively. Top record: $L = 7.4$ with step sizes of 9.1 ± 1.5 nm (slow phase) and 9.0 ± 2.0 nm (fast phase); mean ± s.d. Middle: $L = 17.9$ with step sizes of 7.9 ± 1.3 nm (slow phase) and 8.8 ± 1.5 nm (fast phase). Bottom: $L = 22.0$ with step sizes of 8.5 ± 2.2 nm (slow phase) and 8.8 ± 1.5 nm (fast phase).

Figure S2: 7- and 9-nm stepping data. Mechanical simulation of an alternating 7- and 9-nm stepper. **(a)** Position records of a bead tethered to a microtubule by a single immobilized kinesin molecule as the computer-controlled stage executed 7- and 9-nm steps with times drawn from exponential distributions, thereby simulating kinesin motion with alternating step sizes and experimental noise levels comparable to an experiment with functional kinesin. $F \sim -4$ pN. **(b)** Experimental distribution of step sizes separated by phase. Slow step size = 7.1 ± 0.1 nm and fast step size = 9.3 ± 0.1 nm. Arithmetic mean ± s.e.m. **(c)** Distribution of all step sizes showing a single-Gaussian fit (blue) and double-Gaussian fit (red). Only bins with ≥ 10 counts were included in fits.

APPENDIX

An automated step-finding algorithm implemented in IgorPro 5.0.

Input data: a computer record of position vs. time (typically acquired at 20 kHz, decimated to 2 kHz, and filtered at 1 kHz).

Output data: a list of all successive step sizes.

Key assumption: a nominal (approximate) step size, taken to be 8.2 nm for kinesin (the exact value is not critical).

Algorithm:

1. Smooth the input record of position vs. time using a lowpass boxcar filter (at 0.1-0.5 of the record data rate).
2. Use IgorPro's *Histogram* operation to determine the distribution of positions, using a fine bin size (≤ 1 nm).
3. Use IgorPro's *Derivative* function twice to compute the 2nd derivative (negative peaks reflect dwell positions).
4. Use IgorPro's *FindPeak* operation, with a selected threshold, to create a list of all negative peak locations (i.e., dwell positions).
5. Subtract adjacent dwell positions to generate a list of successive separation distances between events. (Note: if some peaks are missed in step (4), this may return some values that are near integral multiples of the nominal step size.)
6. Using information from the lists created in steps (4) and (5), go back and use IgorPro's *FindLevels* operation, which identifies levels crossing beyond a settable threshold, to identify the final list of times of stepping transitions in the original input record, as follows.
    a. Go systematically through the list generated in step (5), one transition distance (step) at a time.
        i. If this distance is roughly equal to the nominal step size, then set a threshold at the midpoint between the two levels generated in step (4) and apply *FindLevels* with this threshold to identify the transition time.
        ii. If this distance is roughly equal to twice the nominal step size, a (brief) step has likely been missed. In this case, establish two thresholds at ¼ and ¾ of the distance between the levels generated in step (4). Apply *FindLevels* twice, using these thresholds, to identify two nearby transition times.
        iii. If the distance exceeds twice the nominal step size, then flag the event and alert the user not to use this record.
        iv. Verify the transition. To avoid false level crossings (e.g., due to occasional, brief noise spikes in the data), take an average of the input position data on either side of each identified transition to confirm a sustained level change (typically, for 10 ms on either side). If these values differ significantly, the step is verified. If not, then use *FindLevels* with the same threshold to continue searching the input data for the actual transition.

7. Final sanity check: estimate the number of stepping events expected, by dividing the total distance traveled divided by the fundamental step size. Compare this number with the number of steps identified by the algorithm. Alert the user if these numbers differ.
8. Produce final output: find all step sizes within the input record based on the locations of transition times.
    a. Go through the input data record using the list of times generated in step (6), and compute the arithmetic mean for all position values contained within each segment between adjacent, identified transitions.
    b. Generate the list of successive differences from the values identified in step (8a). These are the step sizes.